

AUG 21 1950

Restriction/Classification Cancelled

Copy  
RM L50F22

6

NACA RM L50F22

Inactive

~~SECRET~~  
C.2

~~CONFIDENTIAL~~  
**NACA**

# RESEARCH MEMORANDUM

EFFECT OF AN AUTOPILOT SENSITIVE TO YAWING VELOCITY  
ON THE LATERAL STABILITY OF THE  
DOUGLAS D-558-II AIRPLANE

By Ordway B. Gates, Jr., and Leonard Sternfield

Langley Aeronautical Laboratory  
Langley Air Force Base, Va.

CLASSIFICATION CANCELLED

Authority: NACA R 7.304. Date: 6/10/50

See  
By: *MAA 6/17/50*

Restriction/  
Classification  
Cancelled

This document contains information which, if disclosed, could be injurious to the national defense. It is intended for the use of the Government and its employees only. It is not to be distributed outside the Government or to any person who does not have a legitimate interest therein, and to United States citizens of known loyalty and discretion who of necessity must be informed thereof.

**NATIONAL ADVISORY COMMITTEE  
FOR AERONAUTICS**

WASHINGTON  
August 17, 1950

~~CONFIDENTIAL~~  
Restriction/Classification Cancelled

ERRATA

NACA RM L50F22

EFFECT OF AN AUTOPILOT SENSITIVE TO YAWING VELOCITY ON THE  
LATERAL STABILITY OF THE DOUGLAS D-558-II AIRPLANE

By Ordway B. Gates, Jr., and Leonard Sternfield

August 17, 1950

Page 8, line 17: In the equation for  $(C_n)_{SA}$  the plus sign preceding the term  $(C_l)_{BA} \sin \alpha$  should be changed to a minus sign.

Page 8, next to last equation: The plus sign in the expression  $(C_{n\delta_A} \cos \alpha + C_{l\delta_A} \sin \alpha)$  should be changed to a minus sign.

Page 9:

Line 5: In the first of equations (2) the plus sign in the expression  $(C_{n\delta_A} + \alpha C_{l\delta_A})$  should be changed to a minus sign.

Line 6: In the second of equations (2) the subscript GA on the first term within the brackets should be changed to SA.

Line 10: In the equation for  $\frac{\partial C_n}{\partial (D_b \psi)_{SA}}$  the plus sign preceding the term  $\alpha C_{l\delta_A}$  should be changed to a minus sign.

Line 11: In the equation for  $\frac{\partial C_n}{\partial (D_b \phi)_{SA}}$  the plus sign preceding the term  $\alpha C_{l\delta_A}$  should be changed to a minus sign.

Page 10: In the first two of equations (3) the plus signs preceding the term  $\alpha C_{l\delta_A}$  should be minus signs.

In the first two of equations (5) the term  $(1 - \frac{hc}{l})$  should be  $(1 + \frac{hc}{l})$ .



3 1176 01436 7925

## NATIONAL ADVISORY COMMITTEE FOR AERONAUTICS

## RESEARCH MEMORANDUM

EFFECT OF AN AUTOPILOT SENSITIVE TO YAWING VELOCITY  
ON THE LATERAL STABILITY OF THE  
DOUGLAS D-558-II AIRPLANE

By Ordway B. Gates, Jr., and Leonard Sternfield

## SUMMARY

A theoretical investigation has been made to determine the effect on the lateral stability of the Douglas D-558-II airplane of an autopilot sensitive to yawing velocity. The effects of inclination of the gyro spin axis to the flight path and of time lag in the autopilot were also determined. The flight conditions investigated included landing at sea level, approach condition at 12,000 feet, and cruising at 50,000 feet at Mach numbers of 0.80 and 1.2.

The results of the investigation indicated that the lateral stability characteristics of the D-558-II airplane for the flight condition discussed should satisfy the Air Force - Navy period-damping criterion when the proposed autopilot is installed. Airplane motions in sideslip subsequent to a disturbance in sideslip are presented for several representative flight conditions in which a time lag in the autopilot of 0.10 second was assumed.

## INTRODUCTION

Some recent flight tests of the Douglas D-558-II research airplane have indicated that the lateral oscillation of this airplane is very poorly damped. The results presented in reference 1 show that the damping of the lateral oscillation of an airplane can be improved by use of automatic stabilization. In this investigation the type of autopilot which resulted in the greatest improvement in damping is one which applies rudder control proportional to the yawing angular velocity. Such an autopilot has been installed in the XB-47 and, according to reference 2, the flight tests of this airplane with the autopilot installed indicated an increase in the damping of the lateral oscillation. The purpose of this investigation is to determine the effect of this type of autopilot on the lateral stability of the D-558-II airplane.

A blacked-out redacted area at the bottom of the page.

The effects on the lateral stability characteristics of inclination of the gyro spin axis to the flight path and of time lag in the auto-pilot system are also discussed. The results of the investigation are presented in the form of motions subsequent to an initial disturbance in sideslip and plots of the time to damp to half-amplitude and the period of the oscillation for different flight conditions.

#### SYMBOLS AND COEFFICIENTS

$\phi$	angle of roll, radians
$\psi$	angle of yaw, radians
$\beta$	angle of sideslip, radians ( $v/V$ )
$r, \dot{\psi}$	yawing angular velocity, radians per second ( $d\psi/dt$ )
$p, \dot{\phi}$	rolling angular velocity, radians per second ( $d\phi/dt$ )
$v$	sideslip velocity along lateral axis, feet per second
$V$	airspeed, feet per second
$M$	Mach number
$\rho$	mass density of air, slugs per cubic foot
$q$	dynamic pressure, pounds per square foot ( $\frac{1}{2}\rho V^2$ )
$b$	wing span, feet
$S$	wing area, square feet
$W$	weight of airplane, pounds
$m$	mass of airplane, slugs ( $W/g$ )
$g$	acceleration due to gravity, feet per second per second
$\mu_b$	relative-density factor ( $m/\rho S b$ )
$e$	angle between longitudinal body axis and principal axis, positive when body axis is above principal axis at the nose, degrees

- $\eta$  inclination of principal longitudinal axis of airplane with respect to flight path, positive when principal axis is above flight path at nose, degrees ( $\alpha - \epsilon$ )
- $\gamma$  angle of flight path to horizontal axis, positive in a climb, degrees
- $k_{X_0}$  radius of gyration in roll about principal longitudinal axis, feet
- $k_{Z_0}$  radius of gyration in yaw about principal vertical axis, feet
- $K_{X_0}$  nondimensional radius of gyration in roll about principal longitudinal axis ( $k_{X_0}/b$ )
- $K_{Z_0}$  nondimensional radius of gyration in yaw about principal vertical axis ( $k_{Z_0}/b$ )
- $K_X$  nondimensional radius of gyration in roll about longitudinal stability axis ( $\sqrt{K_{X_0}^2 \cos^2 \eta + K_{Z_0}^2 \sin^2 \eta}$ )
- $K_Z$  nondimensional radius of gyration in yaw about vertical stability axis ( $\sqrt{K_{Z_0}^2 \cos^2 \eta + K_{X_0}^2 \sin^2 \eta}$ )
- $K_{XZ}$  nondimensional product-of-inertia parameter ( $((K_{Z_0}^2 - K_{X_0}^2) \sin \eta \cos \eta)$ )
- $C_L$  trim lift coefficient ( $\frac{W \cos \gamma}{qS}$ )
- $C_l$  rolling-moment coefficient ( $\frac{\text{Rolling moment}}{qSb}$ )
- $C_n$  yawing-moment coefficient ( $\frac{\text{Yawing moment}}{qSb}$ )
- $C_y$  lateral-force coefficient ( $\frac{\text{Lateral force}}{qS}$ )

$$C_{l\beta} = \frac{\partial C_l}{\partial \beta}$$

$$C_{n\beta} = \frac{\partial C_n}{\partial \beta}$$

$$C_{Y\beta} = \frac{\partial C_Y}{\partial \beta}$$

$$C_{n_r} = \frac{\partial C_n}{\partial \frac{rb}{2V}}$$

$$C_{n_p} = \frac{\partial C_n}{\partial \frac{pb}{2V}}$$

$$C_{l_p} = \frac{\partial C_l}{\partial \frac{pb}{2V}}$$

$$C_{Y_p} = \frac{\partial C_Y}{\partial \frac{pb}{2V}}$$

$$C_{Y_r} = \frac{\partial C_Y}{\partial \frac{rb}{2V}}$$

$$C_{l_r} = \frac{\partial C_l}{\partial \frac{rb}{2V}}$$

t

time, seconds

 $s_b$ nondimensional time parameter based on span ( $Vt/b$ ) $D_b$ differential operator  $\left(\frac{d}{ds_b}\right)$ ~~CONFIDENTIAL~~

$P$	period of oscillation, seconds
$T_{1/2}$	time for amplitude of oscillation to damp to one-half its original value
$T_2$	time for amplitude of oscillation to double its original value
$a$	real part of complex root of characteristic stability equation
$\omega$	angular frequency, radians per second
$\omega_s = \frac{b}{V} \omega$	
$\lambda = a \pm i\omega_s$	
$\tau$	time lag between signal for control and its actual motion, seconds
$\delta_A$	deflection of the auxiliary control surface, radians
$C_{n\delta_A}, C_{l\delta_A}$	control effectiveness parameters $\left( \frac{\partial C_n}{\partial \delta_A}, \frac{\partial C_l}{\partial \delta_A} \right)$
$\alpha$	angle of attack with respect to the longitudinal body axis, degrees (See fig. 1.)
$\phi$	inclination of gyro reference axis to the longitudinal body axis, degrees (See fig. 1.)
$\xi$	inclination of gyro reference axis to longitudinal stability or flight-path axis, degrees (See fig. 1.)
$\Delta C_{nr}$	increment of $C_{nr}$ due to the autopilot
$\Delta C_{np}$	increment of $C_{np}$ due to the autopilot
$\Delta C_{lr}$	increment of $C_{lr}$ due to the autopilot
$\Delta C_{lp}$	increment of $C_{lp}$ due to the autopilot

$\dot{\psi}_{GA}$  yawing velocity about an axis perpendicular to the gyro reference axis, radians per second

$$(\dot{\psi}_{GA} = \dot{\psi}_{SA} \cos \xi + \dot{\phi}_{SA} \sin \xi)$$

$$(D_b \dot{\psi})_{GA} = \frac{b}{v} \dot{\psi}_{GA} = D_b \dot{\psi}_{SA} \cos \xi + D_b \dot{\phi}_{SA} \sin \xi$$

K control gearing ratio  $\left( \frac{\partial \delta_A}{\partial \dot{\psi}} \right)_{GA}$

$C_{L\delta_A}$  lift per unit deflection of auxiliary control surface

$\frac{l}{b}$  nondimensional distance from center of gravity of the airplane to center of pressure of the auxiliary control surface

$\frac{h}{b}$  nondimensional distance from airplane longitudinal body axis to center of pressure of the auxiliary control surface

$\frac{S_A}{S_r}$  ratio of auxiliary-control-surface area to rudder area

Subscripts:

GA autopilot, gyro axis

SA stability axis

BA airplane body axis

A auxiliary control surface

#### EQUATIONS OF MOTION

The linearized equations of motion, referred to stability axes, for the condition of controls fixed are:

Rolling

$$2\mu_b (K_X^2 D_b^2 \phi + K_{XZ} D_b^2 \psi) = C_{i\beta} \beta + \frac{1}{2} C_{i_p} D_b \phi + \frac{1}{2} C_{i_r} D_b \psi$$

Yawing

$$2\mu_b (K_Z^2 D_b^2 \psi + K_{XZ} D_b^2 \phi) = C_{n\beta} \beta + \frac{1}{2} C_{n_p} D_b \phi + \frac{1}{2} C_{n_r} D_b \psi$$

Sideslipping

$$2\mu_b (D_b \beta + D_b \psi) = C_{Y\beta} \beta + \frac{1}{2} C_{Y_p} D_b \phi + C_L \phi + \frac{1}{2} C_{Y_r} D_b \psi + (C_L \tan \gamma) \psi$$

When  $\phi_0 e^{\lambda s_b}$  is substituted for  $\phi$ ,  $\psi_0 e^{\lambda s_b}$  for  $\psi$ , and  $\beta_0 e^{\lambda s_b}$  for  $\beta$  in the equations written in determinant form,  $\lambda$  must be a root of the stability equation

$$A\lambda^4 + B\lambda^3 + C\lambda^2 + D\lambda + E = 0 \quad (1)$$

where A, B, C, D, E are defined on pages 7 and 8 of reference 1.

The damping and period of the lateral oscillation in seconds are given by the equations

$$T_{1/2} = \frac{0.693}{a} \frac{b}{V} \quad a < 0$$

$$T_2 = \frac{0.693}{a} \frac{b}{V} \quad a > 0$$

$$P = \frac{6.28}{\omega_s} \frac{b}{V}$$

where  $a$  and  $\omega_s$  are the real and imaginary parts of a complex root of stability equation (1).

Stability derivatives contributed by autopilot.- In order to analyze the effect on the lateral stability of the D-558-II airplane of installing an autopilot sensitive to rate of yaw, the derivation of equations describing the increments to the stability derivatives which must be included in the equations of motion is necessary. The system of axes employed in the derivations is shown in figure 1. Since the equations of motion are derived with respect to the stability axes, the autopilot derivatives must also be related to the stability axes. The autopilot, through use of an auxiliary rudder surface introduces a yawing-moment coefficient about the vertical body axis and a rolling-moment coefficient about the longitudinal body axis, both of which are proportional to the rate of yaw with respect to an axis perpendicular to the gyro reference axis, that is:

$$(C_n)_{BA} = C_{n\delta_A} \delta_A = C_{n\delta_A} \frac{\partial \delta_A}{\partial (D_b \dot{\psi})_{GA}} (D_b \dot{\psi})_{GA}$$

$$(C_l)_{BA} = C_{l\delta_A} \delta_A = C_{l\delta_A} \frac{\partial \delta_A}{\partial (D_b \dot{\psi})_{GA}} (D_b \dot{\psi})_{GA}$$

Now,

$$(D_b \dot{\psi})_{GA} = (D_b \dot{\psi})_{SA} \cos \xi + (D_b \dot{\phi})_{SA} \sin \xi$$

$$(C_n)_{SA} = (C_n)_{BA} \cos \alpha + (C_l)_{BA} \sin \alpha$$

$$(C_l)_{SA} = (C_l)_{BA} \cos \alpha + (C_n)_{BA} \sin \alpha$$

Therefore, by substitution:

$$(C_n)_{SA} = (C_{n\delta_A} \cos \alpha + C_{l\delta_A} \sin \alpha) K \frac{V}{b} \left[ (D_b \dot{\psi})_{SA} \cos \xi + (D_b \dot{\phi})_{SA} \sin \xi \right]$$

$$(C_l)_{SA} = (C_{l\delta_A} \cos \alpha + C_{n\delta_A} \sin \alpha) K \frac{V}{b} \left[ (D_b \dot{\psi})_{SA} \cos \xi + (D_b \dot{\phi})_{SA} \sin \xi \right]$$

where  $K = \frac{\partial \delta_A}{\partial (\dot{\psi})_{GA}}$ . The angles  $\xi$  and  $\alpha$  are assumed to be small. Thus,

the usual simplification is made that the sine of a small angle is equal to the angle in radians, and the cosine is equal to unity. The preceding equations become therefore:

$$\left. \begin{aligned} (C_n)_{SA} &= (C_{n\delta_A} + \alpha C_{l\delta_A})^K \frac{V}{b} \left[ (D_b \psi)_{SA} + \xi (D_b \phi)_{SA} \right] \\ (C_l)_{SA} &= (C_{l\delta_A} + \alpha C_{n\delta_A})^K \frac{V}{b} \left[ (D_b \psi)_{GA} + \xi (D_b \phi)_{SA} \right] \end{aligned} \right\} \quad (2)$$

Equations (2) may be written in the form

$$(C_n)_{SA} = \frac{\partial C_n}{\partial (D_b \psi)_{SA}} (D_b \psi)_{SA} + \frac{\partial C_n}{\partial (D_b \phi)_{SA}} (D_b \phi)_{SA}$$

$$(C_l)_{SA} = \frac{\partial C_l}{\partial (D_b \psi)_{SA}} (D_b \psi)_{SA} + \frac{\partial C_l}{\partial (D_b \phi)_{SA}} (D_b \phi)_{SA}$$

$$\frac{\partial C_n}{\partial (D_b \psi)_{SA}} = K \frac{V}{b} (C_{n\delta_A} + \alpha C_{l\delta_A}) = \frac{1}{2} \Delta C_{nr}$$

$$\frac{\partial C_n}{\partial (D_b \phi)_{SA}} = K \frac{V}{b} (C_{n\delta_A} + \alpha C_{l\delta_A}) \xi = \frac{1}{2} \Delta C_{np}$$

$$\frac{\partial C_l}{\partial (D_b \psi)_{SA}} = K \frac{V}{b} (C_{l\delta_A} + \alpha C_{n\delta_A}) = \frac{1}{2} \Delta C_{lr}$$

$$\frac{\partial C_l}{\partial (D_b \phi)_{SA}} = K \frac{V}{b} (C_{l\delta_A} + \alpha C_{n\delta_A}) \xi = \frac{1}{2} \Delta C_{lp}$$

Thus

$$\left. \begin{aligned}
 \Delta C_{n_r} &= 2K \frac{V}{b} (C_{n\delta_A} + \alpha C_{l\delta_A}) \\
 \Delta C_{n_p} &= 2K \frac{V}{b} (C_{n\delta_A} + \alpha C_{l\delta_A}) \xi = \Delta C_{n_r} \xi \\
 \Delta C_{l_r} &= 2K \frac{V}{b} (C_{l\delta_A} + \alpha C_{n\delta_A}) \\
 \Delta C_{l_p} &= 2K \frac{V}{b} (C_{l\delta_A} + \alpha C_{n\delta_A}) \xi = \Delta C_{l_r} \xi
 \end{aligned} \right\} \quad (3)$$

The control effectiveness parameters,  $C_{n\delta_A}$  and  $C_{l\delta_A}$ , of the auxiliary rudder surface are given by the expressions

$$\left. \begin{aligned}
 C_{n\delta_A} &= -C_{L\delta_A} \frac{S_A}{S} \frac{l}{b} \\
 C_{l\delta_A} &= C_{L\delta_A} \frac{S_A}{S} \frac{h}{b} = -\frac{h}{l} C_{n\delta_A}
 \end{aligned} \right\} \quad (4)$$

Values for the derivative  $C_{L\delta_A}$  were estimated from unpublished theoretical results based on the Weissinger lifting-surface theory. When these expressions for  $C_{n\delta_A}$  and  $C_{l\delta_A}$  are substituted in equations (3) the following equations result:

$$\left. \begin{aligned}
 \Delta C_{n_r} &= -2K \frac{V}{b} C_{L\delta_A} \frac{S_A}{S} \frac{l}{b} \left(1 - \frac{h\alpha}{l}\right) \\
 \Delta C_{n_p} &= -2K \frac{V}{b} C_{L\delta_A} \frac{S_A}{S} \frac{l}{b} \xi \left(1 - \frac{h\alpha}{l}\right) = \xi \Delta C_{n_r} \\
 \Delta C_{l_r} &= -2K \frac{V}{b} C_{L\delta_A} \frac{S_A}{S} \frac{l}{b} \left(\alpha - \frac{h}{l}\right) \\
 \Delta C_{l_p} &= -2K \frac{V}{b} C_{L\delta_A} \frac{S_A}{S} \frac{l}{b} \xi \left(\alpha - \frac{h}{l}\right) = \xi \Delta C_{l_r}
 \end{aligned} \right\} \quad (5)$$

The values of the derivatives  $C_{n_r}$ ,  $C_{n_p}$ ,  $C_{l_r}$ , and  $C_{l_p}$  which appear in the stability equations must be modified therefore to include the increments  $\Delta C_{n_r}$ ,  $\Delta C_{n_p}$ ,  $\Delta C_{l_r}$ , and  $\Delta C_{l_p}$ .

For this investigation a further assumption has been made that the center of pressure of the auxiliary surface is located a negligible distance from the fuselage center line, that is,  $h$  is approximately equal to zero. Also, the product  $\xi\alpha$  is considered to be of second order and terms involving this product have been neglected.

Equations (5) become therefore:

$$\left. \begin{aligned} \Delta C_{n_r} &= -2K \frac{V}{b} C_{L\delta_A} \frac{S_A}{S} \frac{l}{b} \\ \Delta C_{n_p} &= -2K \frac{V}{b} C_{L\delta_A} \frac{S_A}{S} \frac{l}{b} \xi = \xi \Delta C_{n_r} \\ \Delta C_{l_r} &= -2K \frac{V}{b} C_{L\delta_A} \frac{S_A}{S} \frac{l}{b} \alpha = \alpha \Delta C_{n_r} \\ \Delta C_{l_p} &= 0 \end{aligned} \right\} (6)$$

The derivative  $C_{L\delta_A}$  is algebraically positive. Therefore, when  $\xi$  is a negative angle (that is, for the gyro reference axis below the flight path)  $\Delta C_{n_p}$  is positive. Similarly, when  $\alpha$  is negative  $\Delta C_{l_r}$  is positive. It will be shown in a subsequent section entitled "Results and Discussion" that the term  $\Delta C_{l_r}$  has only a negligible effect on the damping of the lateral oscillation of the D-558-II airplane and was therefore omitted in the analysis.

If the location of the auxiliary surface is such as to make the assumption  $h = 0$  invalid, the increments to the stability derivatives should be calculated from equations (5).

## RESULTS AND DISCUSSION

A flight record of the sideslip motion of the D-558-II airplane subsequent to a rudder kick of  $10^\circ$  is shown on figure 2. This flight

was made at an altitude of 12,000 feet and an airspeed of 458 feet per second. The flaps and landing gear were extended. The amplitude of the resulting undamped oscillation is about  $\pm 4^\circ$  and the period is approximately 2.50 seconds.

Calculations were made for this flight condition using the mass and aerodynamic characteristics of reference 3 and from unpublished data to determine whether the roots of the characteristic stability equation (1) would indicate such an undamped oscillation. The results obtained were in good agreement with those of the flight test ( $T_{1/2} = 100$  sec;  $P = 2.5$  sec). The mass and aerodynamic parameters for this flight condition and other conditions to be discussed subsequently are given in table I. Case I in the table represents the flight condition shown on figure 2.

The present investigation was undertaken to determine whether an autopilot sensitive to rate of yaw would satisfactorily improve the poor oscillatory stability characteristics of the D-558-II airplane. If the assumption is made that the autopilot gyro axis is aligned with the longitudinal stability axis the autopilot effectively only introduces the derivative  $\Delta C_{n_r}$ . As indicated in a previous section entitled "Stability derivatives contributed by autopilot," the expression for  $\Delta C_{n_r}$  is a function of two parameters,  $\frac{S_A}{S}$  and the control gearing ratio  $K$ , which may be arbitrarily selected by the designer. Therefore it was first necessary to determine the value of  $\Delta C_{n_r}$  which would give satisfactory lateral stability and then determine the combinations of  $\frac{S_A}{S}$  and  $K$  which would result in that prescribed value of  $\Delta C_{n_r}$ .

The criterion for satisfactory lateral stability as specified by the Air Force and Navy (reference 4) is shown in figure 3. The time required for the amplitude of the oscillation to be reduced to one-half its original value  $T_{1/2}$  is plotted against the period  $P$ . For the flight condition described previously, the value of  $C_{n_r} = -1.0$ . The period-damping relationship of the airplane for this value of  $C_{n_r}$  is located on the unsatisfactory side of the boundary which describes the criterion. The period, as pointed out before, is 2.5 seconds and  $T_{1/2}$  is about 100 seconds. When  $C_{n_r}$  was increased to  $-2.0$ , that is,  $\Delta C_{n_r} = -1.0$ , the period-damping relationship almost exactly satisfied the criterion. For  $\Delta C_{n_r} = -2.0$  the relationship is such as to fall well into the acceptable range. Thus for  $\Delta C_{n_r} = -1.0$  or  $-2.0$ , the period-damping relationship of the D-558-II would be satisfactory.

A theoretical analysis was made therefore to determine the amount of auxiliary area necessary to give these increments of  $C_{n_r}$  for different gearing ratios of the proposed autopilot. The results of this analysis are presented in figure 4. The ratio  $\frac{S_A}{S_r}$  has been used as ordinate instead of  $\frac{S_A}{S}$ .

The combinations of gearing ratio and auxiliary area which would result in a  $\Delta C_{n_r} = -2.0$  for the previously described flight condition (case I) are given by the curve  $\Delta C_{n_r} = -2.0$ . For the gearing ratio of 2 to 1 which was selected for the subsequent analysis, the required area is approximately 20 percent of the rudder. This gearing ratio of 2 to 1 means that the auxiliary surface will be deflected  $2^\circ$  for a  $1^\circ$  per second rate of yaw. For the rates of yaw encountered on this airplane, this is a reasonable value for the gearing ratio. It is important to note that the value of  $\Delta C_{n_r}$  obtained by use of a specific auxiliary surface will be different for other flight conditions since its magnitude varies directly with airspeed. (See equation (6).)

Effect of inclination of the gyro axis.— The assumption was made in the preceding section that the autopilot gyro axis was alined with the flight path or longitudinal stability axis. Since the equations of motion are derived with respect to the stability axes, the autopilot was in effect increasing only the stability derivative  $C_{n_r}$ . For this type of autopilot the angularity between the longitudinal body axis and the gyro spin axis, once fixed, is preserved for all flight conditions and therefore the gyro axis is alined with the flight path for only one angle of attack.

For any flight condition where the gyro axis is not alined with the flight path, that is,  $\xi \neq 0$ , the autopilot is sensitive to both yawing and rolling velocities about the stability axes. Hence an increment to the yawing moment proportional to rolling velocity about the stability axes must also be introduced into the equations of motion. This additional yawing moment due to rolling velocity is in effect an increment in the stability derivative  $C_{n_p}$ .

This derivative  $C_{n_p}$  has been shown to have an important effect on the damping of the lateral oscillation (references 5 and 6). If  $\Delta C_{n_p}$  is algebraically positive it will have a stabilizing effect provided it is not allowed to become excessively large. If  $\Delta C_{n_p}$  becomes too large a positive quantity, another oscillation will be introduced which becomes less stable with further increases in  $\Delta C_{n_p}$ .

Calculations were made for the previously discussed and three other flight conditions, taking into account the derivative  $\Delta C_{np}$ , in order to determine a value for the angle  $\phi$  (see fig. 1) which would be satisfactory throughout the range of likely flight conditions. The mass and aerodynamic parameters for these conditions are given in table I. Numerous values of the angle  $\phi$  were investigated and the results are presented in figure 5. The period of the oscillatory mode P and the time to damp to half amplitude  $T_{1/2}$  in seconds are plotted against the angle  $\phi$  in degrees. For the flight condition at 12,000 feet, figure 5(a), the damping of the original oscillatory mode, denoted by  $(T_{1/2})_1$ , continues to improve as  $\phi$  is increased in the positive direction. The period of this mode, increases slightly as  $\phi$  is increased to  $2^\circ$ , but beyond this value it becomes somewhat less. For  $\phi$  approximately equal to  $2^\circ$  a second oscillatory mode is introduced into the system. The damping and period of this mode are shown as  $(T_{1/2})_2$  and  $P_2$ , respectively. For  $\phi > 2^\circ$  this second oscillation becomes rapidly less stable and for  $\phi > 8^\circ$  this mode is unstable. The period of this second oscillation at first decreases, but for  $\phi > 3^\circ$  the trend is reversed and the period becomes longer for further increases in  $\phi$ . The formation of this second oscillation and its subsequent decrease in stability with increases in  $\phi$  is due to the large positive values of the derivative  $\Delta C_{np}$ . The period of this second oscillation is, in general, much longer than that of the original oscillation.

For the landing condition at sea level, figure 5(b), the damping of the lateral oscillation continues to improve with increases in  $\phi$ , while the period increases only very slightly. For the range of  $\phi$  investigated a second oscillation was not introduced. The results for the subsonic condition at 50,000 feet are shown on figure 5(c). As  $\phi$  is increased, the damping of the original oscillation improves considerably while the period of this oscillation is relatively unchanged. For  $\phi > 5^\circ$  a second oscillation is introduced which becomes rapidly less stable for further increases in  $\phi$ . The period of this mode continues to decrease for the range of  $\phi$  investigated. For the supersonic case at 50,000 feet, figure 5(d), the same trends are noted for the original oscillation. The damping becomes better as  $\phi$  is increased while the period is relatively unchanged. For  $\phi > 5^\circ$ , a second oscillatory mode again is introduced which becomes less stable for larger values of  $\phi$ . From these figures, it appears that the damping of the lateral oscillation will be satisfactory for all the conditions discussed if  $\phi$  is between  $0^\circ$  and  $5.2^\circ$ .

Effect of time lag in the autopilot on the airplane motions.— An experimental frequency-response investigation of the proposed autopilot indicated that it essentially has a constant time lag. The magnitude of this lag was found to be less than 0.10 second. The effect of a time

lag in the autopilot of 0.10 second on the lateral stability of the D-558-II was determined by the methods of reference 7 and found to be negligible. In order to verify this result, the airplane motion in sideslip subsequent to a disturbance in sideslip of  $5^\circ$  was calculated for each of the flight conditions discussed previously taking into account a time lag in the autopilot of 0.10 second. The motions, which were calculated by using a step by step procedure, were obtained for two values of the angle  $\phi$ ,  $-2^\circ$  and  $5^\circ$ , and the results are presented in figure 6. The values of  $T_{1/2}$  and P as determined from these curves are almost identical with the corresponding conditions as shown on figure 5 for which zero time lag was assumed. For  $\phi = 5.2^\circ$ , the presence of a secondary oscillatory mode can be detected in the flight condition at 12,000 feet and in the high-speed case at 50,000 feet. Also, for  $\phi = -2^\circ$ , the damping of the oscillation for the landing condition at sea level and the subsonic case at 50,000 feet barely satisfies the Air Force - Navy criterion.

Effect of  $\Delta C_{l_r}$ .— The autopilot derivative  $\Delta C_{l_r}$  was discussed in a previous section, and in the present analysis was assumed to be negligible. In order to justify this assumption, the motion for  $\phi = 5.2^\circ$  for the subsonic case at 50,000 feet was calculated taking into account the derivative  $\Delta C_{l_r}$  as defined in equations (6). Points on the resulting curve are shown in figure 6 for case III. It is readily seen that the derivative  $\Delta C_{l_r}$  has no effect on the motion for this case.

Additional calculations.— The assumption was made in the previous analysis that the center of pressure of the auxiliary surface was located on the fuselage center line, that is,  $\frac{h}{b} = 0$ . In order to determine the effect of locating the surface at a position above the fuselage center line, some additional calculations were made assuming the center of pressure of the surface to be 6 feet above the fuselage center line ( $\frac{h}{b} = 0.24$ ). Several inclinations of the gyro spin axis were investigated for each of the flight conditions discussed previously and the increments to the stability derivatives  $C_{n_r}$ ,  $C_{n_p}$ ,  $C_{l_r}$ , and  $C_{l_p}$  were calculated from equations (5). A comparison of the values of  $T_{1/2}$  and P obtained for these two center-of-pressure locations is presented in table II. The values of  $\Delta C_{n_r}$  and  $\Delta C_{n_p}$  were assumed to be the same for both center-of-pressure locations for each gyro-axis inclination since the term  $\frac{h\alpha}{l}$  in equations (5) is negligible compared to unity. In general, the results for both center-of-pressure locations show the same trends. For  $\frac{h}{b} = 0.24$  the spiral mode  $(T_{1/2})_1$  is less stable than was indicated by the results

for  $\frac{h}{b} = 0$ . Also, the formation of the second oscillatory mode for each condition investigated occurs at higher values of  $\phi$  for the high center-of-pressure location than for the cases where  $\frac{h}{b} = 0$ . The decrease in spiral stability is due primarily to the large positive values of  $\Delta C_{L_r}$  whereas the delay in the formation of the additional oscillatory mode is due to both the large positive value of  $\Delta C_{L_r}$  and the negative values of  $\Delta C_{L_p}$ . For the values of  $\phi$  which resulted in small values of  $\Delta C_{L_p}$ , the period and damping of the oscillatory mode were only slightly affected, even though  $\Delta C_{L_r}$  was large. For example, the value of  $\Delta C_{L_r}$  for case IV is approximately ten times as large as the  $C_{L_r}$  of the airplane, but for  $\phi = 2^\circ$ , where  $\Delta C_{L_p} = -0.03$ , the only important effect is on the spiral stability. The general effect of locating the surface above the fuselage center line is to shift the curves of figure 5 along the  $\phi$  axis in the positive direction. As a result, the range of  $\phi$  for which the stability of the lateral oscillation will be satisfactory is extended to include higher values of  $\phi$  than for the case of  $\frac{h}{b} = 0$ . For this particular center-of-pressure location, an inclination of the gyro axis of as much as  $10^\circ$  will result in satisfactory stability.

#### CONCLUSIONS

The following conclusions were reached from a theoretical analysis of the effect on the lateral stability of the D-558-II airplane of an autopilot sensitive to rate of yaw:

1. The damping of the lateral oscillation of the D-558-II airplane for all of the flight conditions discussed should satisfy the Air Force - Navy criterion when the proposed autopilot is installed.

2. In analyzing the effect of a rate gyro on lateral stability it is important to take into account the inclination of the gyro spin axis to the flight path. For the case of  $\frac{h}{b} = 0$ , values of  $\phi$  between  $0^\circ$  and  $5^\circ$  will be satisfactory whereas for  $\frac{h}{b} = 0.24$  values up to  $10^\circ$  will result in satisfactory stability.

3. A time lag in the autopilot of 0.10 second had a negligible effect on the calculated lateral stability of the D-558-II airplane.

Langley Aeronautical Laboratory  
National Advisory Committee for Aeronautics  
Langley Air Force Base, Va.

#### REFERENCES

1. Sternfield, Leonard: Effect of Automatic Stabilization on the Lateral Oscillatory Stability of a Hypothetical Airplane at Supersonic Speeds. NACA TN 1818, 1949.
2. White, Roland J.: Investigation of Lateral Dynamic Stability in the XB-47 Airplane. Jour. Aero. Sci., vol. 17, no. 3, March 1950, pp. 133-148.
3. Queijo, M. J., and Michael, W. H., Jr.: Analysis of the Effects of Various Mass, Aerodynamic, and Dimensional Parameters on the Dynamic Lateral Stability of the Douglas D-558-2 Airplane. NACA RM L9A24, 1949.
4. Anon.: Flying Qualities of Piloted Airplanes. U. S. Air Force Specification No. 1815-B, June 1, 1948.
5. Sternfield, Leonard, and Gates, Ordway B., Jr.: A Simplified Method for Determination and Analysis of the Neutral-Lateral-Oscillatory-Stability Boundary. NACA Rep. 943, 1949.
6. Johnson, Joseph L., and Sternfield, Leonard: A Theoretical Investigation of the Effect of Yawing Moment Due to Rolling on Lateral Oscillatory Stability. NACA TN 1723, 1948.
7. Sternfield, Leonard, and Gates, Ordway B., Jr.: A Theoretical Analysis of the Effect of Time Lag in an Automatic Stabilization System on the Lateral Oscillatory Stability of an Airplane. NACA TN 2005. 1950

TABLE I  
 MASS AND AERODYNAMIC CHARACTERISTICS  
 OF THE D-558-II AIRPLANE

	Case I	Case II	Case III	Case IV
Altitude, ft	12,000	0	50,000	50,000
W/S, lb/ft <sup>2</sup>	53	53	53	53
S, ft <sup>2</sup>	175	175	175	175
b, ft	25	25	25	25
$\rho$ , slugs/ft <sup>3</sup>	0.001648	0.002378	0.000361	0.000361
V, ft/sec	458	235	776	1169
Mach number	0.43	0.21	0.80	1.2
l/b	0.80	0.80	0.80	0.80
$\gamma$ , deg	-19.2	0	0	0
C <sub>L</sub>	0.29	0.80	0.49	0.22
$\mu_b$	40	27.7	182	182
K <sub>X</sub> <sup>2</sup>	0.0181	0.0156	0.0156	0.0159
K <sub>Z</sub> <sup>2</sup>	0.153	0.156	0.156	0.155
K <sub>XZ</sub>	-0.0186	0	0.002	-0.006
$\eta$ , deg	-8.5	0	0.85	-2.55
$\epsilon$ , deg	5.2	5.2	3.35	3.35
C <sub>Lp</sub> , per radian	-0.33	-0.30	-0.33	-0.33
C <sub>Lr</sub> , per radian	0.37	0.35	0.23	0.15
C <sub>np</sub> , per radian	0.22	-0.05	-0.05	-0.01
C <sub>nr</sub> , per radian	-0.984	-0.77	-0.69	-0.67
C <sub>yp</sub> , per radian	0	0	0	0
C <sub>yr</sub> , per radian	0	0	0	0
C <sub>y<math>\beta</math></sub> , per radian	-0.79	-0.59	-0.58	-0.57
C <sub>n<math>\beta</math></sub> , per radian	0.41	0.29	0.25	0.23
C <sub>l<math>\beta</math></sub> , per radian	-0.23	-0.17	-0.18	-0.11
$\phi$ , deg	Variable	Variable	Variable	Variable
$\xi$ , deg	Variable	Variable	Variable	Variable
$\alpha$ , deg	-3.3	5.2	4.2	0.80
K	2	2	2	2
C <sub>n<math>\delta_A</math></sub> , per radian	-0.027	-0.027	-0.027	-0.027
$\frac{S_A}{S_r}$	0.20	0.20	0.20	0.20

TABLE II  
 COMPARISON OF PERIOD AND TIME TO DAMP TO ONE-HALF AMPLITUDE FOR TWO  
 CENTER-OF-PRESSURE LOCATIONS OF THE AUXILIARY SURFACE

$\frac{h}{b} = 0; \Delta C_{Lr} = \Delta C_{Lp} = 0$						$\frac{h}{b} = 0.24$								
Case	$\phi$	$\Delta C_{nr}$	$\Delta C_{np}$	$(T_{1/2})_1$	$(T_{1/2})_2$	Oscillations			$(T_{1/2})_1$	$(T_{1/2})_2$	Oscillations		$\Delta C_{Lr}$	$\Delta C_{Lp}$
						$T_{1/2}$	$T_2$	P			$T_{1/2}$	P		
I	-2.0	-1.98	0.045	1.50	0.26	1.06		2.80	3.48	0.24	1.29	2.52	0.71	-0.016
	2.0	↓	.183	---	---	{.63 .64		{9.34 3.74}	3.14	.25	1.07	2.73	↓	-.065
	6.0	↓	.321	---	---	{3.92 .36		{7.06 3.09}	2.67	.26	.89	3.03	↓	-.115
	10.2	↓	.466	---	---	.32	4.22	{8.28 2.65}	---	---	1.25 .38	{11.56 4.18}	↓	-.167
II	-2.0	-1.01	-.127	3.24	.32	4.50		3.27	5.24	.34	3.83	3.20	.21	.027
	5.2		0	2.70	.34	3.20		3.50	4.69	.34	2.77	3.44	0	
	10.2		.089	2.26	.37	2.80		3.60	4.04	.35	2.15	3.60		-.019
III	-2.0	-3.35	-.363	3.91	.43	4.10		2.83	5.20	.45	9.65	2.95	.76	.08
	2.0	↓	-.129	2.64	.58	2.17		2.98	4.09	.52	3.15	3.12	↓	.029
	6.0	↓	.105	---	---	{1.41 1.30}		{21.5 3.13}	2.87	.67	1.72	3.33	↓	-.024
	10.2	↓	.351	---	---	{3.58 .86		{11.75 3.12}	---	---	1.60 1.02	{27.8 3.6}	↓	-.08
IV	-2.0	-5.05	-.247	4.12	.30	.97		2.45	8.5	.38	.96	2.30	1.44	.071
	2.0	↓	.106	2.18	.57	.61		2.63	6.82	.44	.70	2.49	↓	-.03
	6.0	↓	.458	---	---	{2.78 .42		{12.75 2.51}	5.20	.55	.52	2.72	↓	-.13
	10.2	↓	.810	---	---	.36	9.0	{12.9 2.3}	2.61	1.25	.40	3.83	↓	-.23



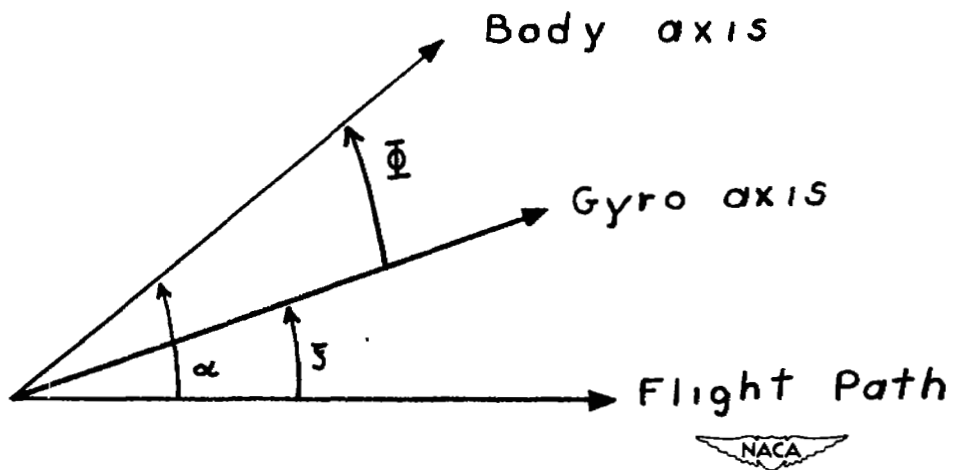


Figure 1.- System of axes used in analysis of stability derivatives contributed by autopilot. Arrows denote positive directions.

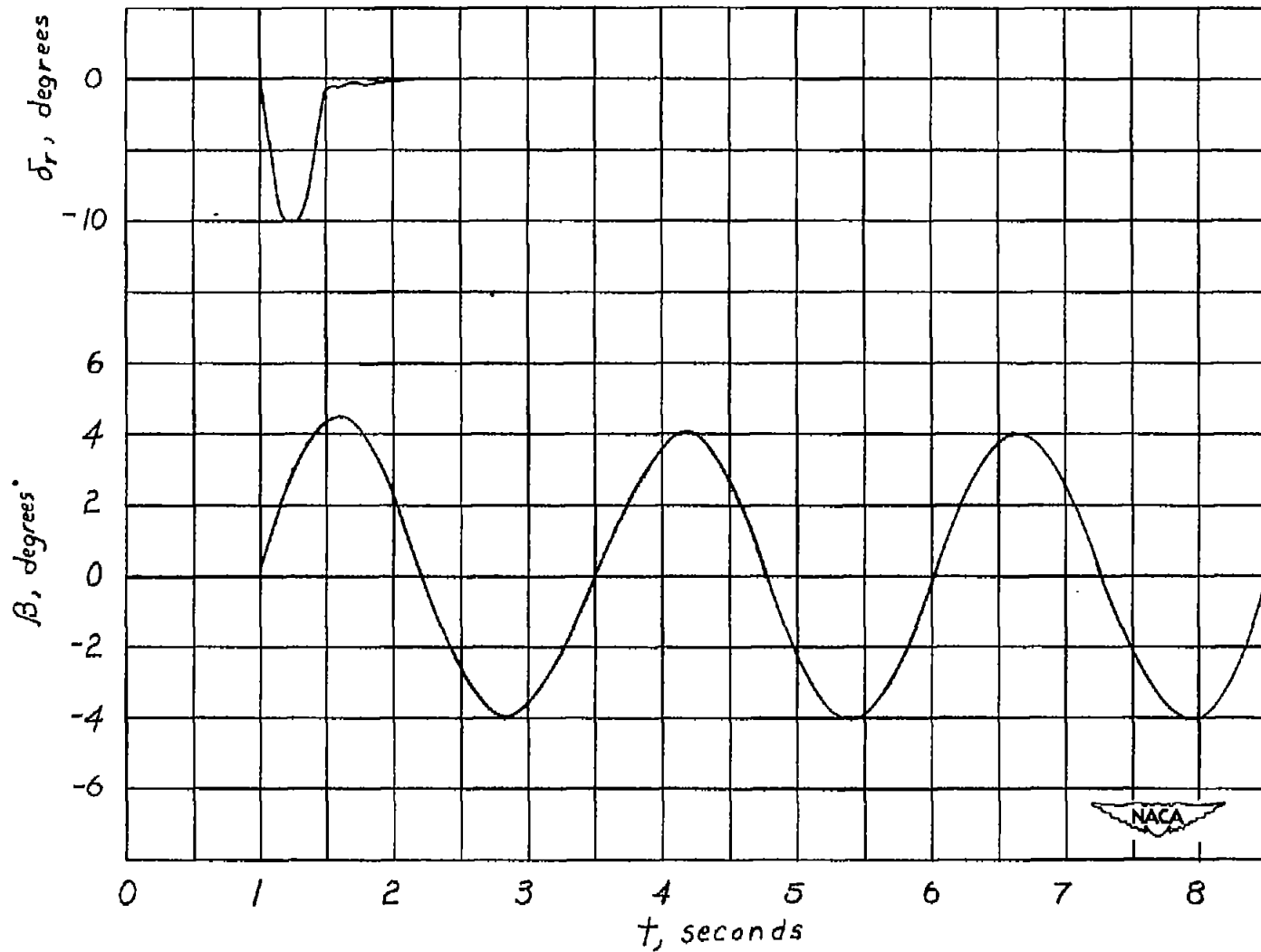


Figure 2.- Motion in sideslip of the D-558-II airplane as indicated by a flight test made at 12,000 feet, flaps and gear down,  $C_L = 0.29$ .

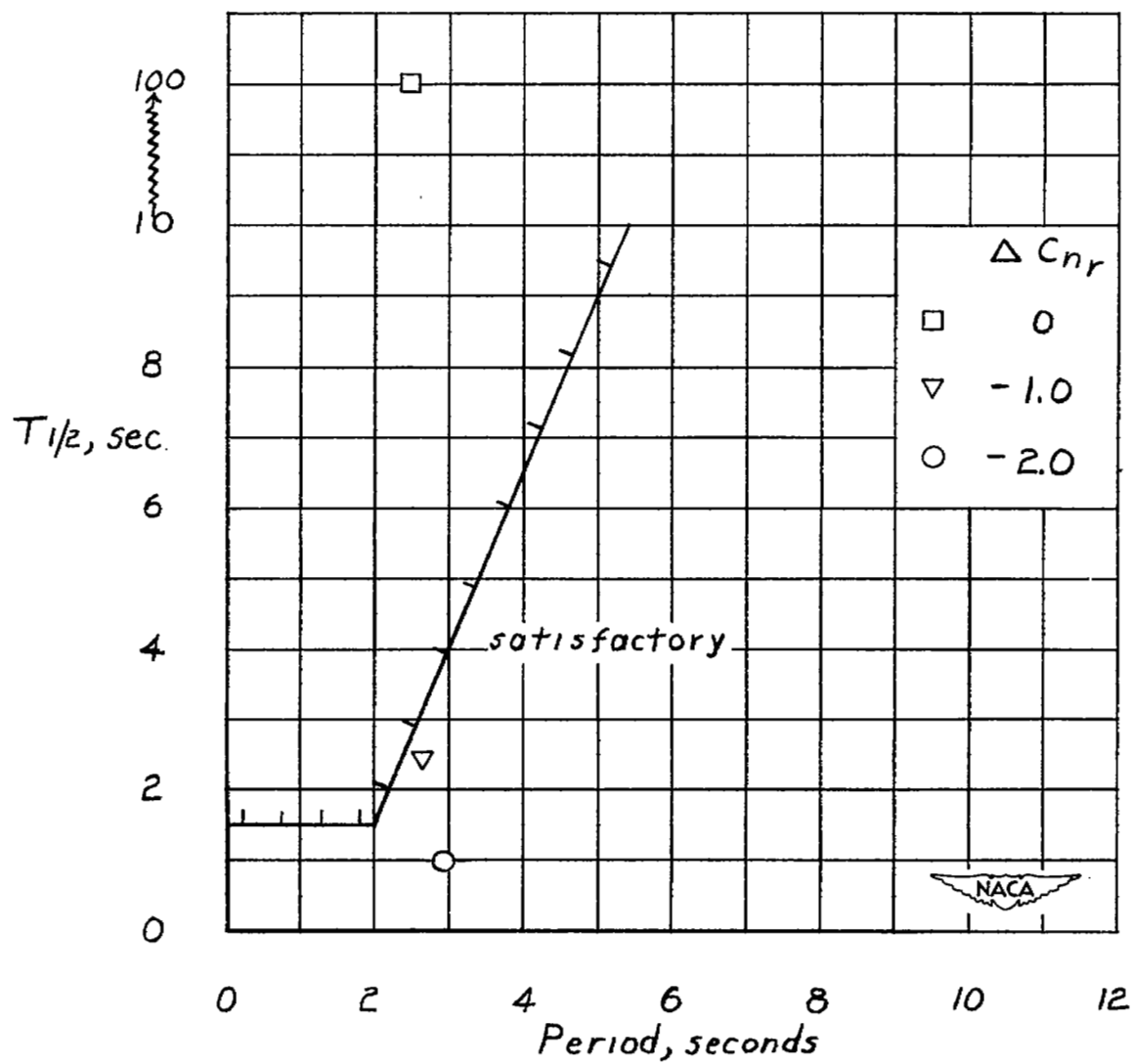


Figure 3.- Effect of  $C_{nr}$  on the damping of the lateral oscillation of the D-558-II airplane. Condition I. (See table I.)

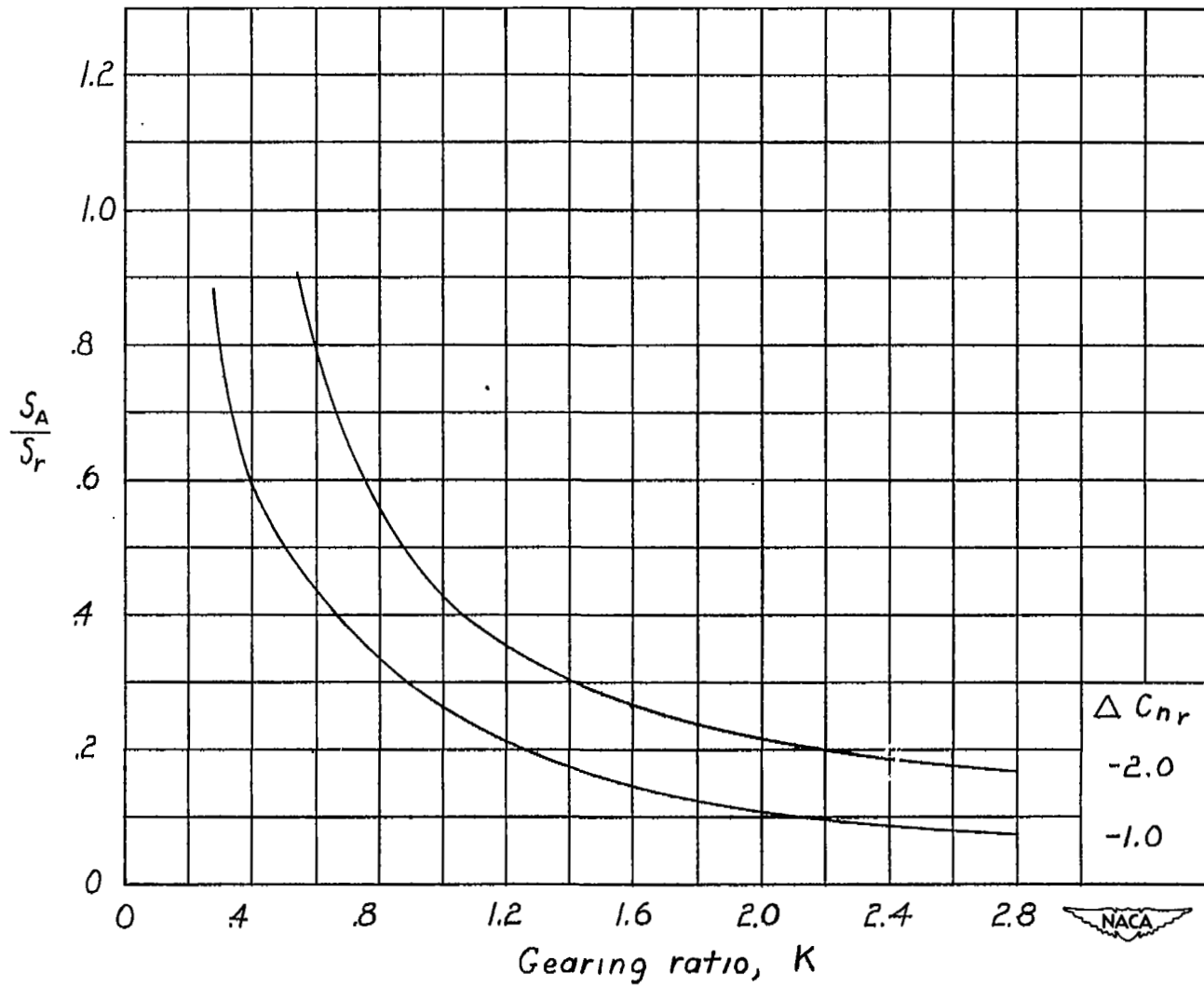
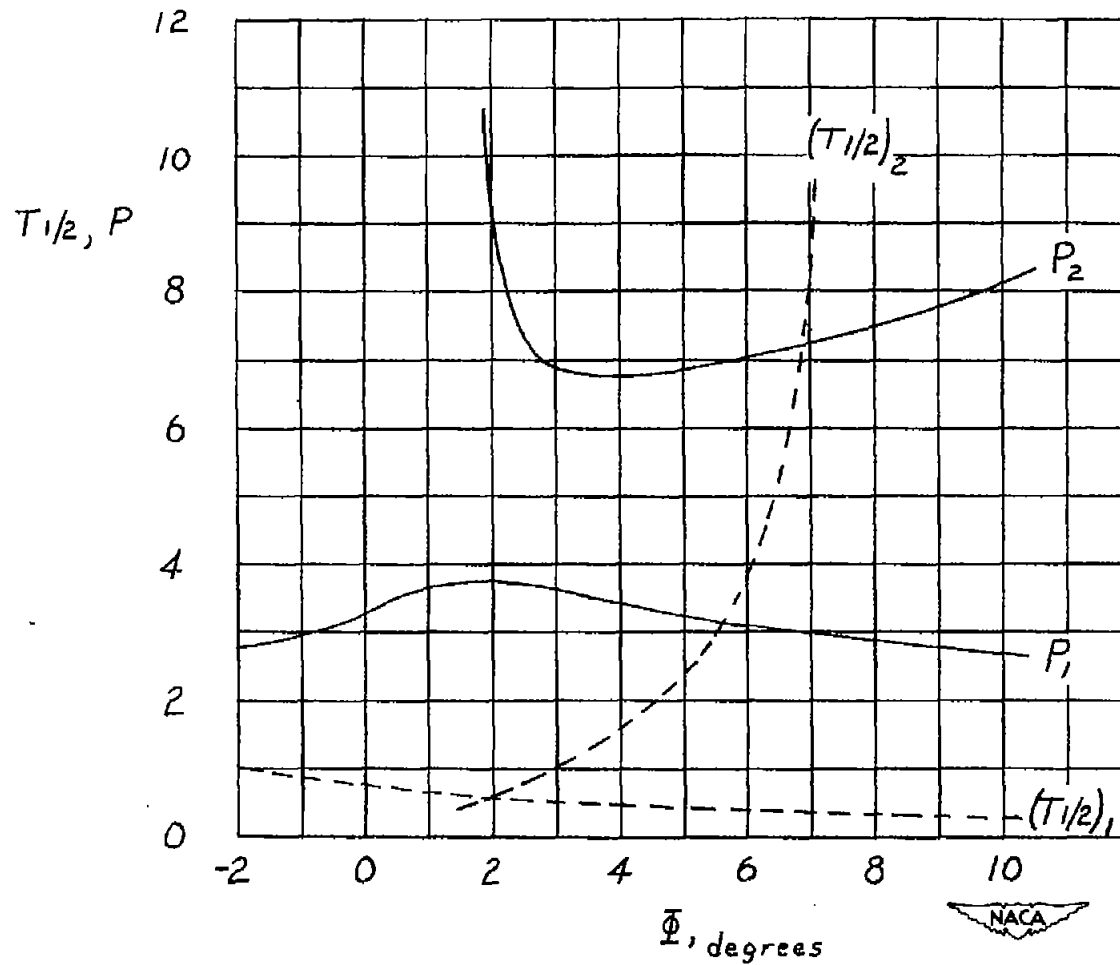
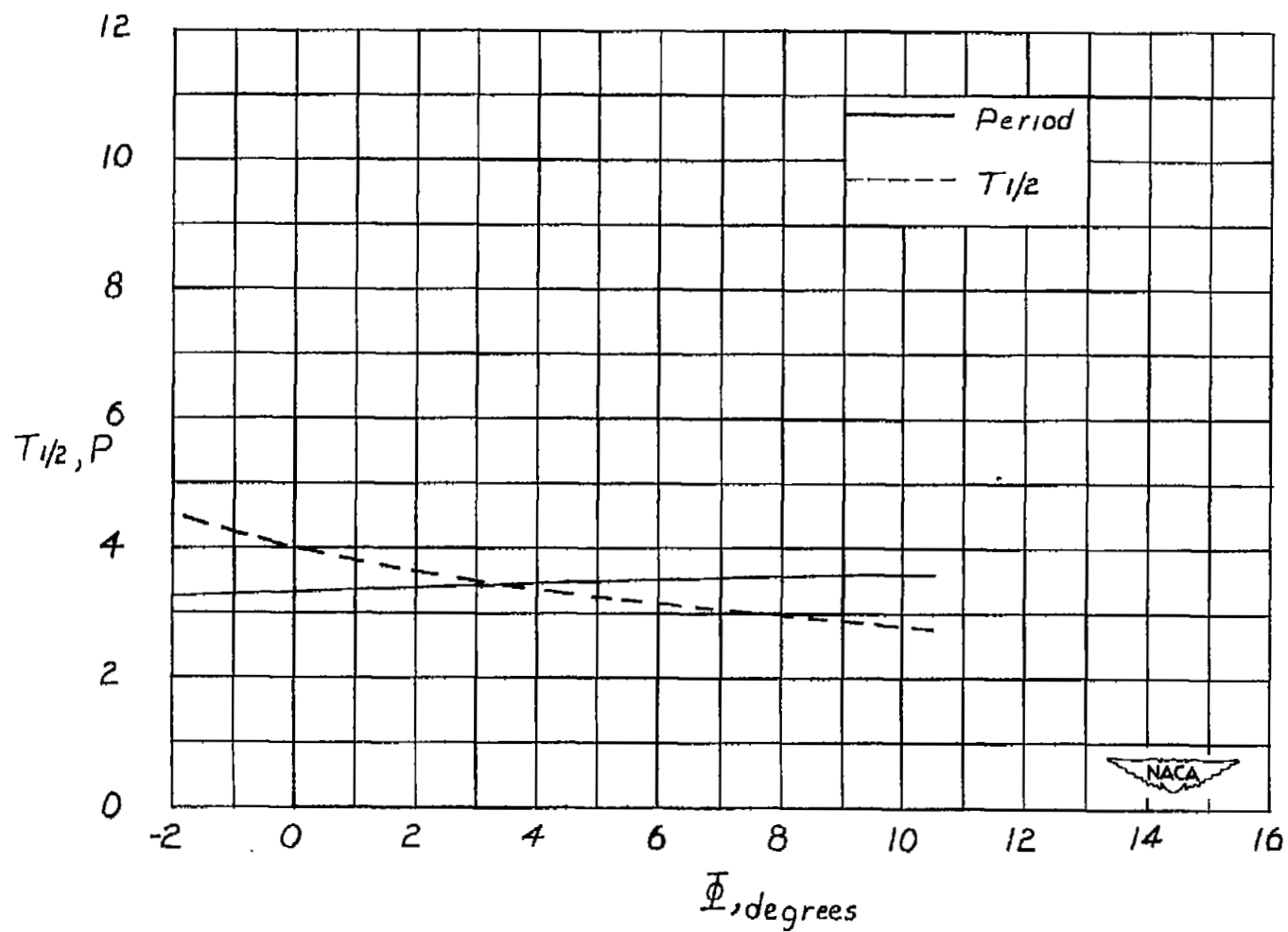


Figure 4.- Combinations of auxiliary surface area and autopilot gearing ratios necessary to obtain various amounts of  $\Delta C_{nr}$ .



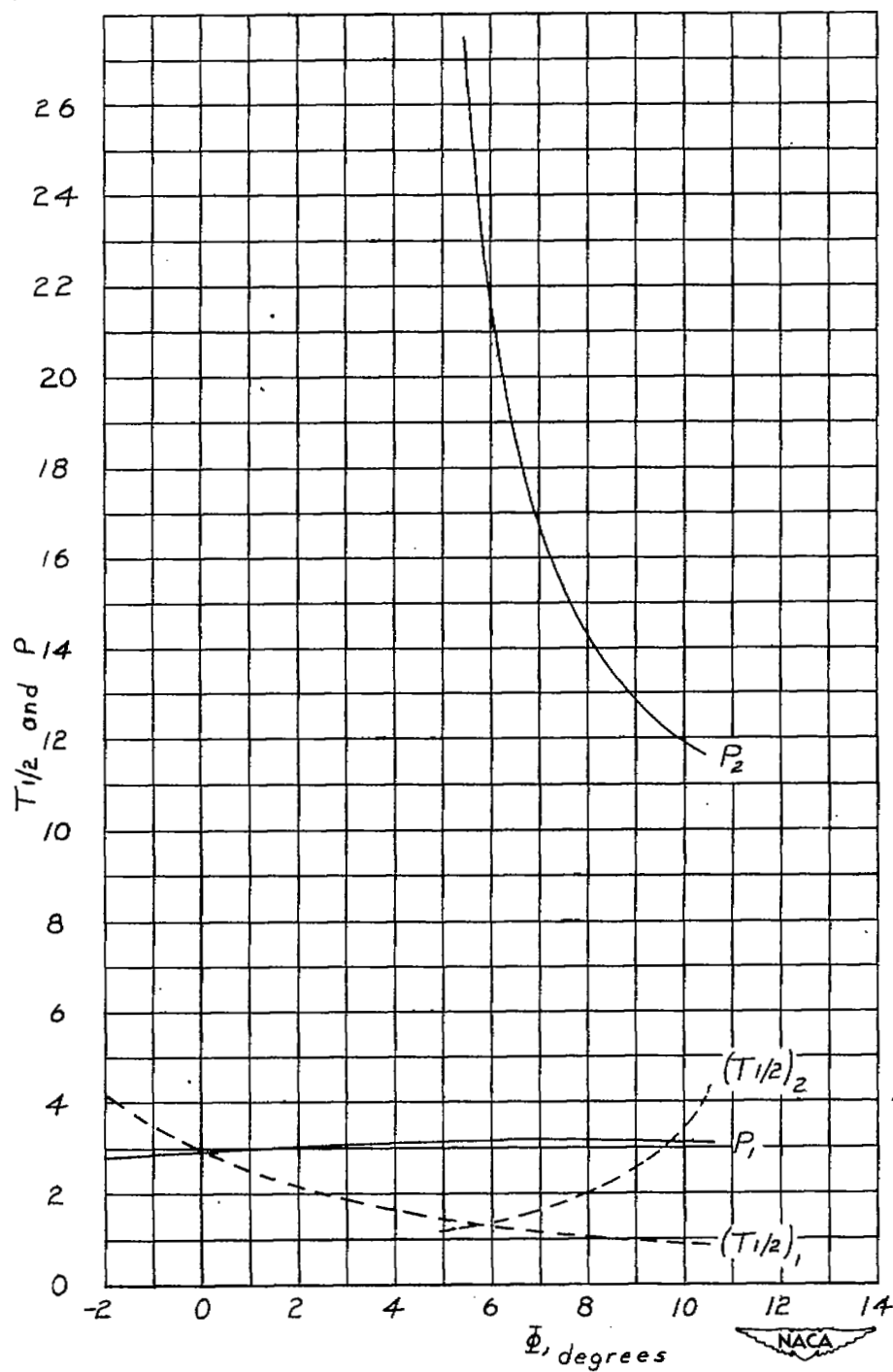
(a) Flight condition I. (See table I.)

Figure 5.- Variation of period and damping of the lateral oscillation of the D-558-II with autopilot gyro axis inclination.



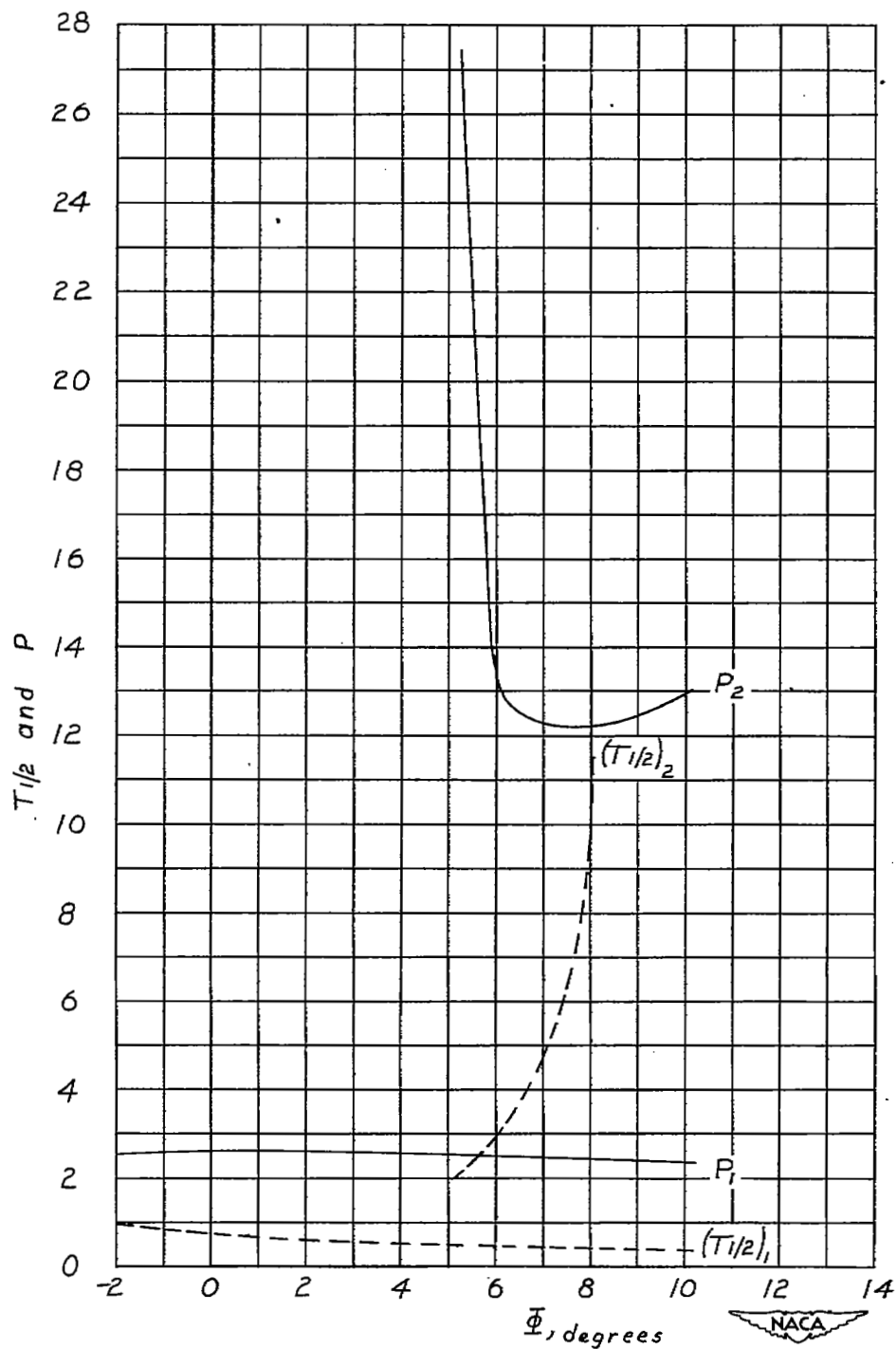
(b) Flight condition II. (See table I.)

Figure 5.- Continued.



(c) Flight condition III. (See table I.)

Figure 5.- Continued.



(d) Flight condition IV. (See table I.)

Figure 5.- Concluded.

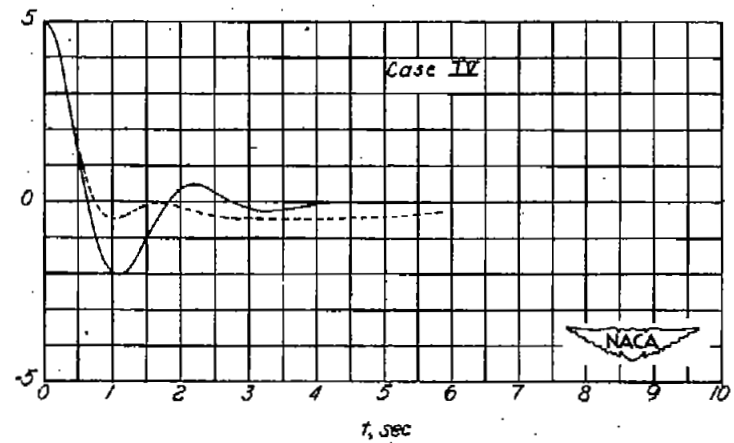
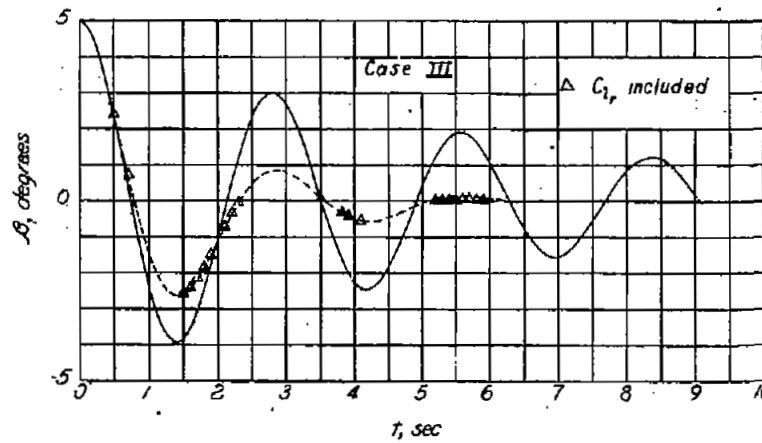
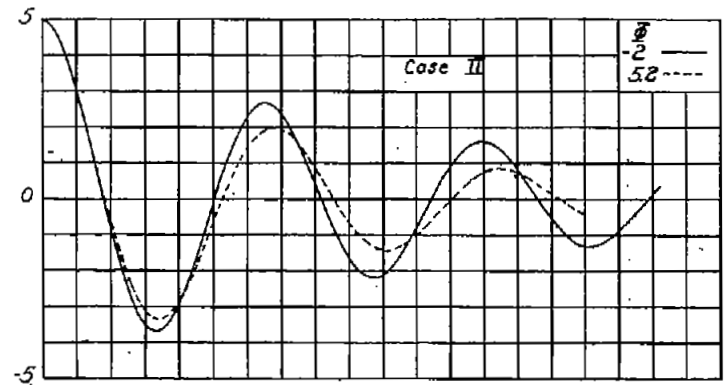
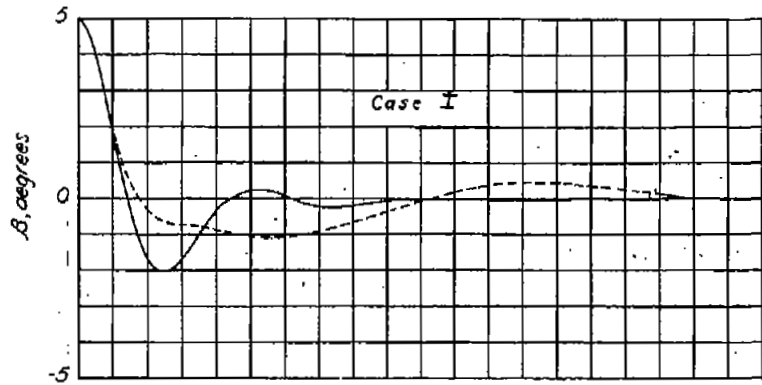


Figure 6.- Airplane motions in sideslip for several representative flight conditions.  $\tau = 0.10$  second.

NASA Technical Library



3 1176 01436 7925



7